IOSR Journal of Electronics and Communication Engineering (IOSR-JECE)
e-ISSN: 2278-2834,p- ISSN: 2278-8735.Volume 13, Issue 2, Ver. II (Mar. - Apr. 2018), PP 82-88
www.iosrjournals.org

Reflexive Spotting of the Deep Vein Thrombosis in the Femoral Nerve Using RF Classifier Model

Anita Titus[1], Nirmaladevi R[2]
[1,2](*Department of ECE, Agni College of Technology,India)*
Corresponding Author: Anita Titus

Abstract: *A nerve that arises from the second, third and fourth lumbar nerves and supplies the muscles and skin of the anterior region of the thigh is known as femoral nerve. It is the main nerve that extends to the knee muscles. The damage of this nerves affects the walking ability of a human. This paper proposes a real-time image are collected from the public database. As the collected images are more prone to noise, they are preprocessed. The preprocessed images are next segmented by Active Contour Method. From the segmented images, shape and texture features such as area, eccentricity solidity, perimeter, major axis length, contrast, correlation. Energy and homogeneity are extracted. Feature extraction helps to select the relevant attributes for classifying and detecting the affected areas. The images are classified as malignant or benign using Random Forest Classifier. Performance indices such as sensitivity, specificity and accuracy were computed.*
Keywords-*Active Contour Method, Deep Vein Thrombosis, Random Forest Classifier.*

Date of Submission: 14-04-2018 Date of acceptance: 30-04-2018

I. Introduction

This article focuses on detecting the femoral vein thrombosis in the femoral vein. The femoral vein runs along the legs from groin area downwards. An ultrasound with a blood clot visible in the left common femoral vein is shown in the figure 1. Some of the symptoms of femoral vein thrombosis includes, tenderness along the veins, noticeable swelling of the entire leg, calf of the affected leg may swell to a size that is more than 3 centimeters greater than the nonaffected leg, etc. A survey shows that in 77.5% of the cases the femoral nerve was located within 5mm of the femoral artery. The rest were located more than 5mm lateral of the artery.

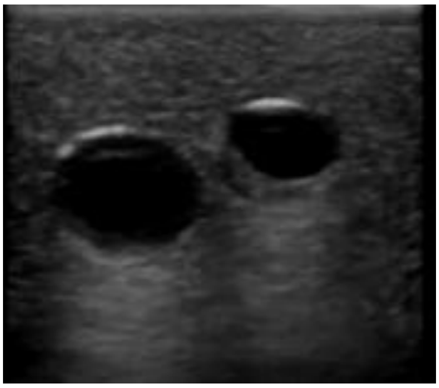

Figure 1. An ultrasound with a blood clot visible in the left common femoral vein

This paper proposes a real-time detection algorithm for deep vein thrombosis of the femoral nerve. Initially a real-time image is collected from the database and is analyzed by applying preprocessing techniques. Further the preprocessed images are segmented by Active Contour Method (ACM) [6],[8] and their features like area, eccentricity, solidity, perimeter, major axis length, contrast, correlation, energy and homogeneity are extracted using feature extraction. Finally, the images are classified by using Random Forest classifier.

Literature review: *A.R. Abdel-Dayemet al [1]*has introduced a fully automated segmentation scheme for carotid artery ultrasound images. The proposed scheme is based on fuzzy c-means clustering. It consists of four major stages. These stages are pre-processing, feature extraction, fuzzy c-means clustering, and finally boundary extraction. Experimental results demonstrate the efficiency of the proposed scheme in segmenting carotid artery ultrasound images. This paper has proposed a scheme for extracting the carotid artery contour using ultrasound images. The proposed scheme uses the fuzzy c-means clustering algorithm to cluster the image pixels into three classes, representing the area inside the artery, the artery wall and the surrounding tissues.

P.Abolmaesumi et al[2] presents a real-time technique to extract the boundary of the carotid artery from ultrasound images. A star algorithm is used to track the center of the carotid artery and its stability is increased by using a temporal Kalman filter. A spatial Kalman filter is used to estimate the carotid artery boundary. The idea comes from the well-known problem of tracking a single tar-get in a randomly distributed cluttered environment. Since the method does not employ any numerical optimization, convergence is very fast.

*P. Abolmaesumi et al [3]*presents a novel segmentation technique for extracting cavity contours from ultrasound images. The problem is first discretized by projecting equispaced radii from an arbitrary seed point inside the cavity toward its boundary. The convergence rate of the method is very fast because it does not employ any numerical optimization. The robustness and accuracy of the method are demonstrated by segmenting contours from a series of ultrasound images. The results are validated through comparison with manual segmentations performed by an expert. An application of the method in segmenting bone contours from computed tomography images is also presented.

*W.S. Beattie et al [4]*aims to present a postoperative cardiac morbidity and mortality continue to pose considerable risks to surgical patients. The use in high-risk cardiac patients remains controversial. No study has shown that postoperative epidural analgesia decreases postoperative myocardial infarction (PMI) or death. All studies are underpowered to show such a result, and the cost of conducting a large trial is prohibitive. Metaanalysis is performed to determine whether postoperative epidural analgesia continued for more than 24 h after surgery reduces PMI or in-hospital death. Metaanalysis was conducted by using the fixed-effects model, calculating both an odds ratio and a rate difference. Postoperative epidural analgesia resulted in better analgesia for the first 24 h after surgery. The rate of PMI was 6.3%, with lower rates in the Epidural group (rate difference, -3.8%; 95% confidence interval [CI] -7.4%, -0.2%; P = 0.049). The frequency of in-hospital death was 3.3%, with no significant difference between Epidural and Nonepidural groups (rate difference, -1.3%; 95% CI, -3.8%, 1.2%, P = 0.091).

V.W.Chan et al [5] Regional anesthesia for outpatient hand surgery can result in shorter recovery times and faster hospital discharge after surgery. These attributes may reduce the demand on nursing time and hospital cost. Potential disadvantages are longer induction time and technique-related failure that might increase operating room time. Unlike previous retrospective reviews, the present study prospectively examined three anesthetic techniques, namely general anesthesia, IV regional anesthesia, and axillary brachial plexus block, with respect to clinical outcome, time efficiency, and hospital cost. This study has demonstrated the potential impact of anesthetic techniques on recovery time, but time savings may not represent true cost savings.

*A. Blake et al [6]*proposed a method for tracking visual contours is described. A new learning algorithm has been described for live tracking of moving objects from video. It supplies dynamics, modelled by a stochastic differential equation, to be used predictively in a contour tracker. The process is bootstrapped by a default tracker which assumes constant-velocity rigid motion driven randomly. It is crucial that the constraints of rigid body motion are incorporated-represented in algorithm by the Q-space. This is what allows stable tracking, for which the number of free parameters must be limited, to be combined with the apparently conflicting requirement that many control points are needed for accurate shape representation.

*J. Guerrero et al [7]*proposed a method for vessel segmentation and tracking in ultrasound images using Kalman filters is presented. A modified Star–Kalman algorithm is used to determine vessel contours and ellipse parameters using an extended Kalman filter with an elliptical model. To calculate the transverse vessel area vessel contour and ellipse parameters are used. A temporal Kalman filter is used for tracking the vessel center over several frames, using location measurements from a handheld sensorized ultrasound probe. The segmentation and tracking have been implemented in real-time and validated using simulated ultrasound data with known features and real data, for which expert segmentation was performed. Results indicate that mean errors between segmented contours and expert tracings are on the order of 1%–2% of the maximum feature dimension, and that the transverse cross-sectional vessel area as computed from estimated ellipse parameters, as determined by the algorithm is within 10% of that determined by experts. The location of the vessel center was tracked accurately for a range of speeds from 1.4 to 11.2 mm/s.

*.J. Guerrero et al [8]*proposed a system for deep venous thrombosis for objective vessel compression and characterization using ultrasound image data and ultrasound probe. A modified star-Kalman algorithm is used for feature detection in acquired ultrasound images, and objective measures of vessel compressibility are calculated from the detected features and acquired force and location data from the sensorized probe. The compressibility measures were validated using expert segmentation of healthy and diseased vessels and compared using paired t-tests, which showed a significant difference between healthy and diseased cases for both measures. 100% sensitivity and specificity were obtained for both measures. The system was implemented in real-time (16 Hz) and evaluated using a tissue phantom and on healthy human subjects. Sensitivity was 100%

and 60%, while specificity was 97% for both measures when implemented. The initial results for the system and its components are promising.

*A.Lasso et al [9]*proposed a variety of advanced image analysis methods that have been under development for ultrasound-guided interventions. The objective of the paper is to provide a freely available opensource software platform—PLUS: Public software Library for Ultrasound—to facilitate rapid prototyping of ultrasound-guided intervention systems for translational clinical research. PLUS also explains about the performance in ultrasound-guided intervention systems. The essential requirements for the development of ultrasound-guided intervention systems is fulfilled by PLUS. It is widely used in translational research prototyping platform.

*Titus et al [10]*aims to present CAD (Computer Aided Diagnosis) helps to detect the Interstitial Lung Diseases(ILDs) like emphysema, ground glass opacity, fibrosis and micro nodules based on the texture analysis of lung. Initially, the image is sent to training data set and test data test and it is segmented. In this paper, Gray Level Histogram(GLH) are used to extract the texture feature and PSO are used for optimization wavelet feature extraction. Quincunx Wavelet Transform(QWT) is applied to the lung region. Support Vector Machine (SVM) classifier is used as a classifier to classify the different lung tissue patterns.

II. Methods

This section first collects an ultrasound image from a database to detect the thrombosis in the femoral vein. Next, preprocessing is an important step in image analysis process to eliminate the noise from image. Then, Active Contour Method (ACM) [6], [8] is applied to segment the affected region from unaffected region and their features are extracted. Finally, Random Forest classifies the image as either benign or malignant. The block diagram of the proposed system is shown in the below figure 2.

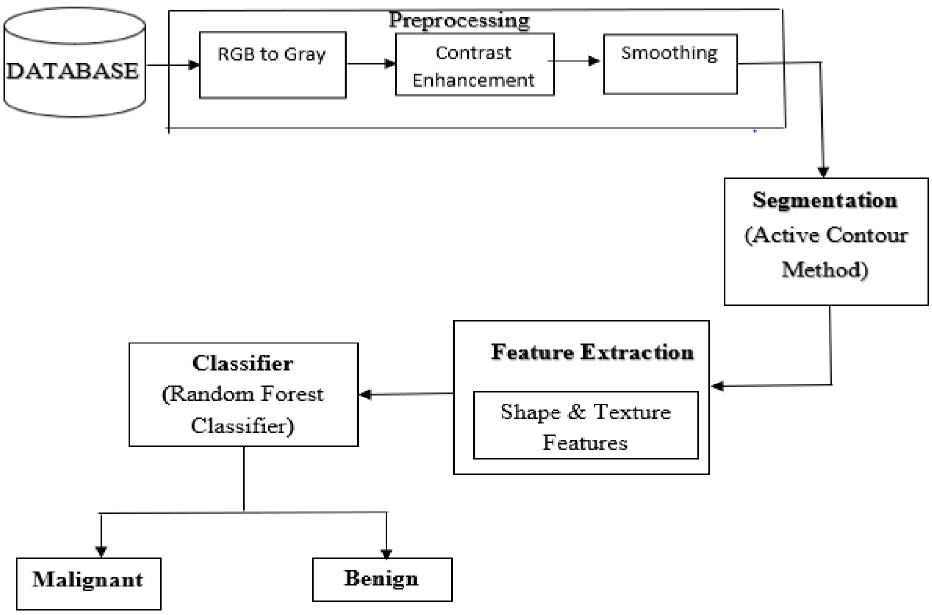

Figure 2. Block diagram of the proposed system

A. Preprocessing

Input:

Ultrasound images collected from public database are the input.

Process:

Step 1: Convert the ultrasound RGB image to a gray scale image.

Step 2: Apply histogram equalization to the gray scale image.

Step 3: Apply Gaussian filter to the histogram equalized image and resize the image to 320*400 pixels.

Output:

The output of the preprocessing module is the denoised image.

The block diagram and steps involved in the preprocessed image are shown in the figures 3&4.

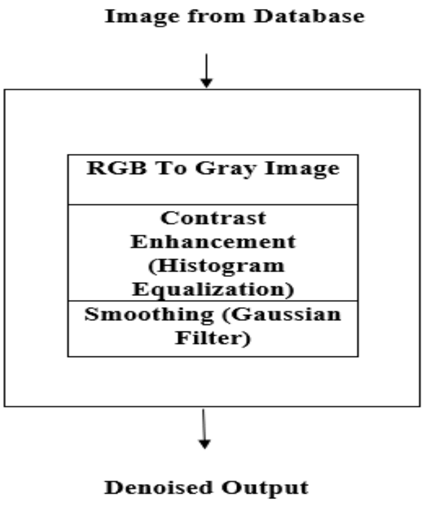

Figure 3. Block diagram of preprocessing module

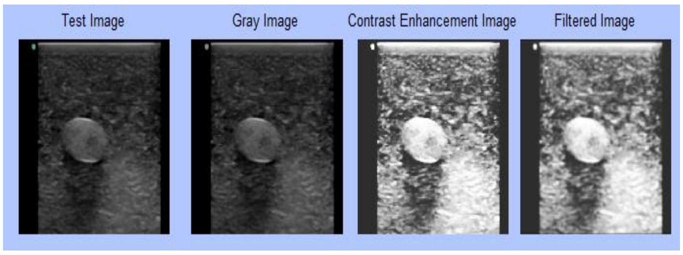

Figure 4. Preprocessed image

B. Segmentation

Input:
Grayscale Gaussian filtered denoised image.
Process:
Step 1: Segment the thrombosis region into right and left side.
Step 2: Create the initialization mask for the right side of the image.
Step 3: Resize the image using the initialization mask.
Output: Segmented the affected region.
The final segmented image is shown in the figure 5.

Figure 5. Final Segmented Image

C. Feature Extraction

The features are extracted from the segmented image. Consider Pij is the element i,j of the normalized symmetrical GLCM(Gray Level Co-occurrence Matrix), N is the number of gray levels in the images, μ is the GLCM mean,$\boldsymbol{\sigma}^2$ is the variance of the intensities of all the reference pixels in the relationship that contributed to GLCM and C is the correlation features.
Input:
Segmented image affected by blood clot.

Process:
Step 1: Compute the 'area' feature which is the actual number of pixels in an image.
Step 2: Compute the 'eccentricity' feature that is a scalar value of the ellipse that specifies the ratio of the distance between the foci of the ellipse and major axis length.
Step 3: Compute the 'solidity' feature which is a scalar value that specifies the proportion of pixels in the convex hull that are also present in ROI using eqn (3.1),

$$\textbf{Solidity} = \frac{\textbf{Area}}{\textbf{Convex Area}} \quad \textbf{(3.1)}$$

Step 4: Compute the 'Major Axis Length' feature that has the same normalized second central moments as the region, returned as a scalar.
Step 5: Compute the 'Perimeter' feature that is a scalar value of the distance between each adjoining pair of pixels around the border of the region.
Step 6: Compute the 'Contrast' feature is the element difference moment of order II, which has a relatively low value when the high values of P are near the main diagonal using eqn (3.2),

$$\boldsymbol{Contrast} = \sum_{i,j=0}^{N-1} \boldsymbol{Pij}(\boldsymbol{i}-\boldsymbol{j})^2 \quad \textbf{(3.2)}$$

Step 7: Compute the 'Correlation' feature that measures the linear dependency of gray levels of neighboring pixels using eqn (3.3),

$$\boldsymbol{Correlation} = \sum_{i,j=0}^{N-1} \boldsymbol{Pij} \frac{(i-\square)(j-\square)}{\sigma^2} \quad \textbf{(3.3)}$$

Step 8: Compute the 'Energy' feature which is the highest value when all values in the co-occurrence matrix are all equal using eqn (3.4),

$$\boldsymbol{Energy} = \sum_{i,j=0}^{N-1} (\boldsymbol{Pij})^2 \textbf{(3.4)}$$

Step 9: Compute the 'Homogeneity' feature that measures the closeness of the distribution of elements in the gray level matrix and helps in better segmentation using eqn (3.5),

$$\boldsymbol{Homogeneity} = \sum_{i,j=0}^{N-1} \frac{\boldsymbol{Pij}}{1+(i-j)^2} \quad \textbf{(3.5)}$$

Output: Nine shape and texture features are computed.

D. Classification
The extracted features are next used for classification. The database consists of 62 ultrasound images of which 53 are malignant and 9 are benign. Totally 14 test images are taken to identify the type of images in which 11 are malignant and 3 are benign. Some of the malignant and benign images are shown in the figures 6&7.

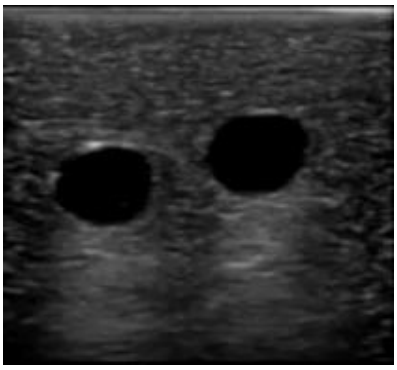

Figure 6. Malignant image

Figure 7. Benign image

III. Results & Discussions

The system was implemented using MATLAB GUI interface. Using Gaussian filter, the noise is filtered from the enhanced image. The filtered image is then re-sized 320*400 pixels. The next step is the segmentation which is used to detect the blood clot in the femoral nerve. Active contour method is used for the segmentation process. Then the features like shape and texture are extracted from the segmented image. In this work, nine different features such as area, eccentricity, solidity, major-axis length, perimeter, contrast, correlation, energy and homogeneity are extracted. The last process is classification. Random forest classifier is used to classify the image as benign or malignant. If the value of the class is '0'it is called benign else it is called malignant. The simulation result using MATLAB is shown in the figure 8.

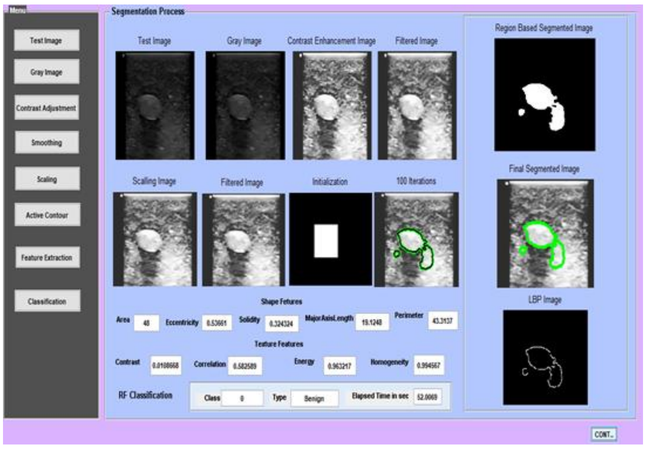

Figure 8. Simulation results using MATLAB

The performance indices such as 58% Sensitivity and 100% specificity were obtained. The execution time of the proposed system is 0.487669sec and its accuracy is 95%. The overall system performance evaluation is shown in figure 9.

Figure 9. Overall system performance evaluation

IV. Conclusion

The active contour technique has many advantages and some disadvantages like determining initial points of the contour, type of the image and, computing difficulty, as well. This method automatically tracks the blood clot in femoral nerve and it is more convenient for clinicians when compared to other methods. ACM is employed to segment Deep Vein Thrombosis in the ultrasound image of femoral nerve. For the segmentation method, active contour method will segment clot in the femoral nerve. Using less accurate but satisfactory techniques it is possible to low the computing difficulty and the option of the initial points of the contour can be automatized. It is known that these methods have an accuracy of 95%. Here, multiple blood clots are difficult to detect. Future work includes segmenting more than one blood clot in the femoral nerve.

References

[1]. A.R. Abdel-Dayem and M.R. El-Sakka, "Fuzzy C-means clustering for segmenting carotid artery ultrasound images," Image Anal. Recognit., pp. 935–948, 2007.

[2]. P. Abolmaesumi, M. Sirouspour, and S. Salcudean, "Real-time extraction of carotid artery contours from ultrasound images," in Proc. 13th IEEE Symp. Comput. -Based Med. Syst., 2000, pp. 2–7.

[3]. P. Abolmaesumi and M. R. Sirouspour, "An interacting multiple model probabilistic data association filter for cavity boundary extraction from ultrasound images," IEEE Trans. Med. Imag., vol. 23, no.6, pp. 772–784, Jun. 2004.

[4]. W.S. Beattie, N.H. Badner, and P. Choi, "Epidural analgesia reduces post-operative myocardial infarction: A meta-analysis," Anaesthesia Analgesia, vol. 93, pp. 853–858, 2001.

[5]. V.W. Chan et al., "A comparative study of general anesthesia, intravenous regional anesthesia, and axillary block for outpatient hand surgery: Clinical outcome and cost analysis," Anesthesia Analgesia, vol. 93, pp. 1181–1184, 2001.

[6]. A. Blake, M. Isard, and D. Reynard, "Learning totrackthe visual motion of contours," Artif. Intell., vol. 78, no. 1–2, pp. 179–212, 1995.

[7]. J. Guerrero, S.E. Salcudean, J.A. McEwen, B.A. Masri, and S. Nicolaou, "System for deep venous thrombosis detection using objective Compression measures," IEEE Trans. Biomed. Eng., vol.53, no.5, pp. 845–854, May 2006.

[8]. J. Guerrero, S.E. Salcudean, J.A. McEwen, B.A. Masri, and S. Nicolaou, "Real-time vessel segmentation and tracking for ultrasound imaging applications," IEEE Trans. Med. Imag., vol. 26, no. 8, pp. 1079–1090, Aug. 2007.

[9]. A. Lasso, T. Heffter, A. Rankin, C. Pinter, T. Ungi, and G. Fichtinger, "PLUS: Open-source toolkit for ultrasound-guided intervention systems," IEEE Trans.Biomed. Eng., vol.61, no.10, pp. 2527-2537, Oct. 2014.

[10]. Anita Titus, H. Khanna Nehemiah and A. Kannan "Classification of Interstitial Lung Diseases Using Particle Swarm Optimized Support Vector Machine" International Journal of Soft Computing 10(1): 25-36, Jan. 2015.

IOSR Journal of Electronics and Communication Engineering (IOSR-JECE) is UGC approved Journal with Sl. No. 5016, Journal no. 49082.

Anita Titus "Reflexive Spotting of the Deep Vein Thrombosis in the Femoral Nerve Using RF Classifier Model." IOSR Journal of Electronics and Communication Engineering (IOSR-JECE) 13.2 (2018): 82-88.